Applied Surface Science 303 (2014) 250–254

Contents lists available at ScienceDirect

Applied Surface Science

journal homepage: www.elsevier.com/locate/apsusc

Nano sized bismuth oxy chloride by metal organic chemical vapour deposition

Pravin Jagdale[a,*], Micaela Castellino[b], Françoise Marrec[c], Sandra E. Rodil[d], Alberto Tagliaferro[a]

[a] Department of Applied Science and Technology (DISAT), Politecnico di Torino, 10129, Italy
[b] Center for Space Human Robotics, Istituto Italiano di Tecnologia, Corso Trento 21, 10129 Torino, Italy
[c] Laboratory of Condensed Matter Physics, University of Picardie Jules Verne (UPJV), Amiens 80039, France
[d] Instituto de Investigaciones en Materiales, Universidad Nacional Autonoma de Mexicom (UNAM), Mexico D.F. 04510, Mexico

ARTICLE INFO

Article history:
Received 24 November 2013
Received in revised form 21 February 2014
Accepted 24 February 2014
Available online 12 March 2014

Keywords:
Nano structure
Crystal structure
X-ray diffraction
Metal organic chemical vapor deposition
Bismuth compound
Nano material

ABSTRACT

Metal organic chemical vapour deposition (MOCVD) method was used to prepare thin films of bismuth based nano particles starting from bismuth salts. Nano sized bismuth oxy chloride (BiOCl) crystals were synthesized from solution containing bismuth chloride ($BiCl_3$) in acetone (CH_3—CO—CH_3). Self-assembly of nano sized BiOCl crystals were observed on the surface of silicon, fused silica, copper, carbon nanotubes and aluminium substrates. Various synthesis parameters and their significant impact onto the formation of self-assembled nano-crystalline BiOCl were investigated. BiOCl nano particles were characterized by X-ray diffraction, X-ray photoelectron spectroscopy, field emission scanning electron microscopy, energy-dispersive X-ray spectroscopy and Micro-Raman spectroscopy. These analyses confirm that bismuth nanometer-sized crystal structures showing a single tetragonal phase were indeed bismuth oxy chloride (BiOCl) square platelets 18–250 nm thick and a few micrometres wide.

1. Introduction

Increased environmental concerns and the need for 'green reagents' have tremendously fostered the interest on bismuth and its compounds in the last decade [1]. Bismuth and its compounds have been used as the active components in some medical preparations [2]. Bismuth is the heaviest stable element on the periodic table. In spite of its heavy metal status, bismuth is considered to be safe, as it is non-toxic and non carcinogenic [1]. This is at odds with other elements close to it in the periodic table such as arsenic, antimony, lead and tin, which are highly toxic and pose environmental hazards [3]. Bismuth compounds such as bismuth oxy chloride (BiOCl) are relatively non-toxic, easy to handle and can tolerate small amounts of moisture [4].

Moreover, BiOCl is an important ternary compound due to the coexistence of unique and excellent optical, catalytic, electrical, magnetic and luminescence properties [5–8]. BiOCl with a band gap of 3.5 eV, is used as a pigment in cosmetic industry [9,10], which is a potential photocatalyst under UV light irradiation [11,12] and can compete with TiO_2 in this respect [13]. In 2009, Lee et al. [14] also reported that a BiOCl/Bi_2O_3 hetero-junction acts as a new visible light photocatalyst. It has been used as a catalyst for the oxidative cracking of hydrocarbons and also used as photoluminescent material [6] and for thermally stimulated conductivity. The outstanding properties of Bismoclite (BiOCl) can be obviously enhanced using 2D nanoplates and nanosheets because of their large surface-to-volume ratios.

Processes commonly employed to grow BiOCl nanometer-size metal particles are electrochemical [15], facile hydrolysis [16,17], flame spraying [18], inert gas condensation [19], laser ablation in solution [20], solution phase chemical methods [21–24], wet chemical [25], reduction of relevant metal salts [22,23], hydrothermal process [26] and thermal decomposition of organometallic precursors [24]. However, these methods require complex processes and the use of toxic and highly sensitive agents, which can hardly be scaled for industrial purposes. In this paper, we reported about a one-step metal organic chemical vapour deposition (MOCVD) method to grow bismoclite nanocrystallites thin films in platelet form. This method is more suitable due to green chemistry approach, environmentally less hazardous, chemically and commercially viable and possible to scale up from lab to

* Corresponding author at: Department of Applied Science and Technology (DISAT), Politecnico di Torino, C.so Duca degli Abruzzi, 24, 10129 Torino, Italy. Tel.: +39 011 5647347; fax: +39 0174 560861.
E-mail address: pravin.jagdale@polito.it (P. Jagdale).

http://dx.doi.org/10.1016/j.apsusc.2014.02.158
0169-4332/

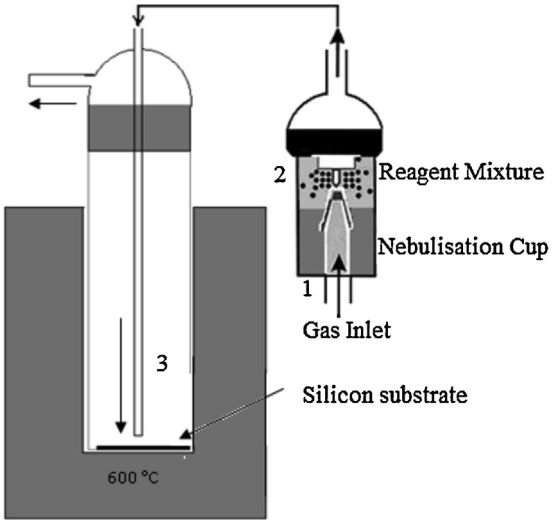

Fig. 1. Schematic representation of MOCVD setup.

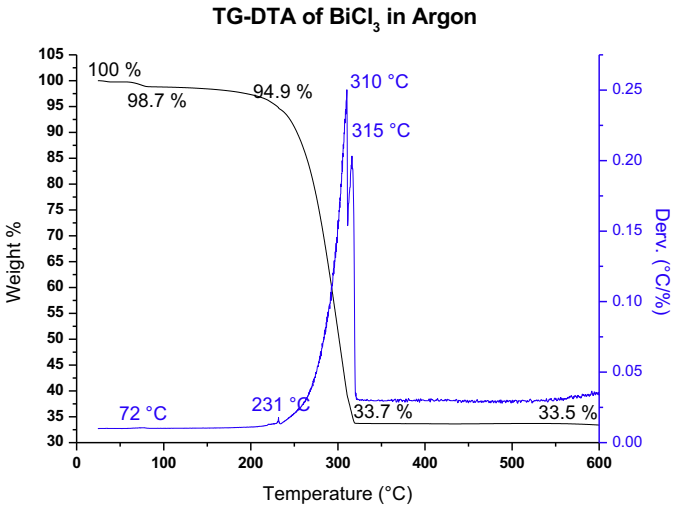

Fig. 2. TG-DTA analysis of $BiCl_3$ in Argon.

industrial scale. As mentioned above, the growth was achieved on a variety of silicon substrates such as silicon (1 0 0), silicon (1 1 1) and polycrystalline silicon carbide (SiC).

2. Experimental

Bismuth based nanoparticles were grown starting from a dispersed solution of bismuth salt [27,28]. Synthesis was performed by a MOCVD process. MOCVD was selected because it is one of the best methods for depositing thin layers with precisely controlled thickness and it is easy-to-scale up. In MOCVD, the metal organic precursor is evaporated and spread over the substrate hot surface in an inert atmosphere. The temperature in the furnace is regulated so that the metal organic molecules dissociate, depositing the metal atoms on the surface, layer by layer. By varying the experimental conditions and type of substrate, it is possible to tailor the properties of the crystals at the atomic scale. Bismuth chloride ($BiCl_3$) (Aldrich, 98% purity) was used as bismuth and chlorine atomic source for synthesizing nano particles of BiOCl. Acetone (Erba, 99.8% purity) was used as a solvent to dissolve $BiCl_3$ and convert it to solution form. The reagent mixture was prepared by continuous stirring of 0.1 g of $BiCl_3$ in 10 ml of acetone for at least 10 min.

MOCVD experimental setup (Fig. 1) contains a cylindrical, flat bottom glass vessel with a diameter of 50 mm and a depth of 300 mm. This shape was selected to achieve better thermal contact between the bottom of the glass vessel and the substrate lower surface. The reactor top consists of inlet and outlet glass tubes for gases. The inlet gas tube is designed in such a way that it carries the reacting gas flux directly on the substrate. The distance between the tube edge and the substrate is set at 10 mm. Furnace hosts 120 mm of the glass reactor length inside the heating zone. A 400 sccm nitrogen/argon flow rate is maintained during deposition, in order to provide an inert atmosphere and a laminar gas flow to transport solution into the reaction chamber. Different crystalline orientations of optically flat surface silicon i.e., silicon (1 0 0), silicon (1 1 1) and polycrystalline silicon carbide (Si-C) (Si-MAT, Germany) were used to study the deposition of bismuth based nanoparticles (BiNPs). A solvent compatible plastic humidifier cup (Fig. 1) was used as solution container. Inert gas flow was inserted from the bottom (Fig. 1, label 1) of the humidifier cup. Nebulization technique was adopted to mobilize a liquid homogeneous mixture to carry over the substrate inside the reactor. The inert gas flow rate was increased through the nozzle (Fig. 1, label 2) placed inside the humidifier cup.

The first step of the process was to get rid of residual air by means of a pure argon gas flow. Then the furnace was brought at thermal equilibrium at the required deposition temperature (600 °C). In the furnace, the high temperature leads to the pyrolysis of the gas mixture that ultimately led to the nano particles thin film growth on the substrate. When the growth process ended, the furnace was allowed to cool down to room temperature while keeping an inert gas flow. Deposits of BiNPs were found both on the inner tube wall and on the substrates (Fig. 1).

BiNPs morphology, chemical composition and thermal decomposition were studied by Field emission scanning electron microscope (FE-SEM) equipped with energy dispersive spectroscopy (EDS), X-ray diffraction (XRD), Thermo gravimetry analyses (TGA) and X-ray photoelectron spectroscopy (XPS).

3. Result and discussion

3.1. Thermo gravimetric analysis (TGA)

In order to highlight the path that leads from $BiCl_3$ precursor to BiNPs in the MOCVD process, changes in physical and chemical properties of materials as a function of increasing temperature (with constant heating rate 10 °C/min) in Ar atmosphere was studied by the TGA. Both weight loss and its derivative are plotted in Fig. 2. As temperature increases gradually, the first weight loss (1.3%) is observed at 72–100 °C and is related to moisture. The second weight loss (3.8%) is observed at 231 °C and is attributed to the melting of $BiCl_3$ [10]. The most relevant weight loss (61.2%) is peaked at 310–315 °C. It is attributed to the breaking of $BiCl_3$ and subsequent formation of BiNPs. After 320 °C no weight loss was observed, indicating the formation of stable BiNPs (33.5%). So the major chemical transformation from $BiCl_3$ salt to BiNPs takes place between 250 and 350 °C.

3.2. Field emission scanning electron microscopy-energy dispersive spectroscopy (FESEM-EDS)

BiNPs (Table 1) appear in the form of rectangular or square shaped walls/platelets with sharp edges, hence we term them bismuth based nano walls (BiNWs). Inter connectivity among BiNWs is very good due to the merging of neighbouring nano-walls. The thickness of the single nano wall was different depending on the substrate used; for the Si (1 0 0) varied in the range 44–240 nm. While, the thickness of BiNWSs grown on the silicon (1 1 1)

Table 1
FESEM of the BiNWs on Silicon (100), Silicon (111), Polycrystalline Silicon carbide (SiC).

Analysis	Silicon (100)	Silicon (111)	Silicon carbide(SiC)
FESEM	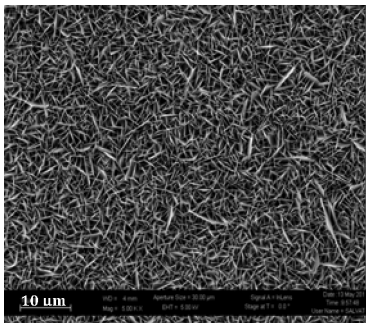	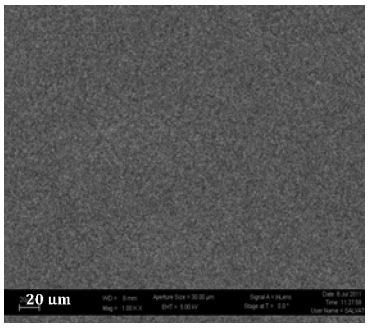	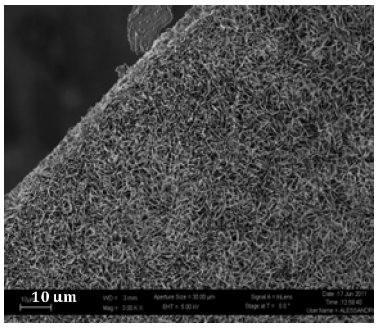
Thickness measurement of crystals	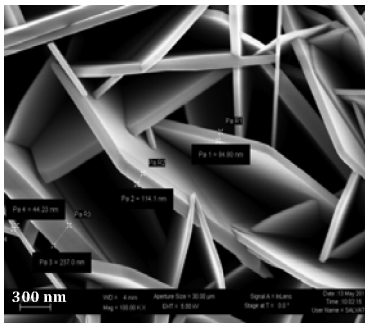	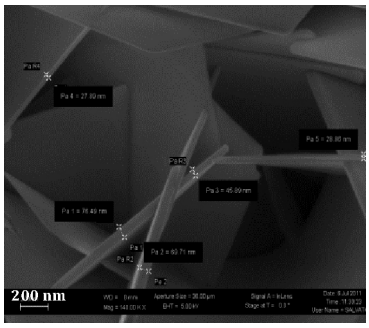	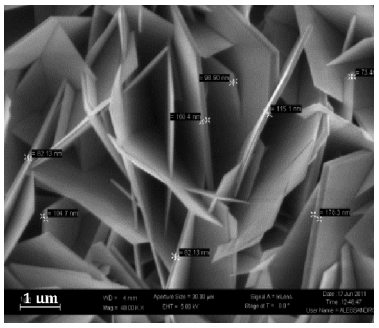
EDS spectrum analyzed area	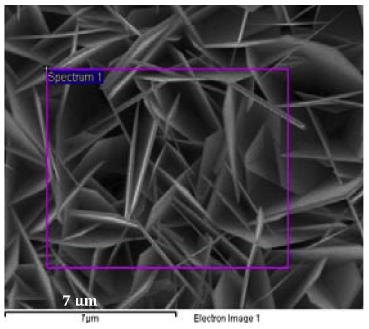	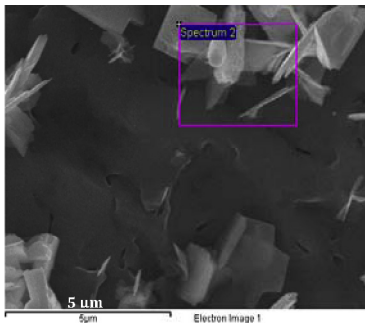	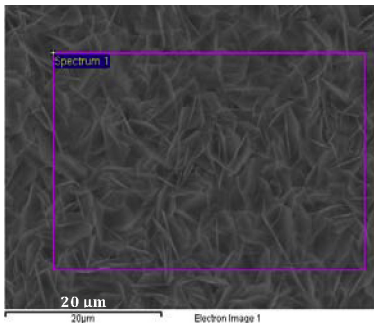

surface was in the range of 25–77 nm and on SiC surface in the range 70–180 nm. Similar BiNWs were observed on other substrates too. The total thickness of the film formed by BiNWs on silicon (1 0 0) surface is ~5.2 μm.

Table 2 shows the quasi-stoichiometric composition obtained on all the silicon substrates. The weight ratio among Bi:Cl:O reported in the literature is: Bi – 80.24, Cl – 13.62, O – 6.14 [29]. We assume (as a working hypothesis at this stage) that our BiNWs are actually BiOCl nanowalls (BiOClNWs). In silicon (1 1 1) elemental wt.% composition varies with respect to two other substrates due to selection of spectrum zone in EDS. That excess amount of chlorine and oxygen comes from the bare silicon (1 1 1) surface.

3.3. Low laser power Micro-Raman

The low laser power Micro-Raman spectrum of BiOClNWs shows (Fig. 3) the presence of peaks at ~143 cm^{-1} and 200 cm^{-1}, which are characteristic peaks of the BiOCl [30], confirmed by measurements on stoichiometric BiOCl powders (provided by Farmaquimia, Mexico).

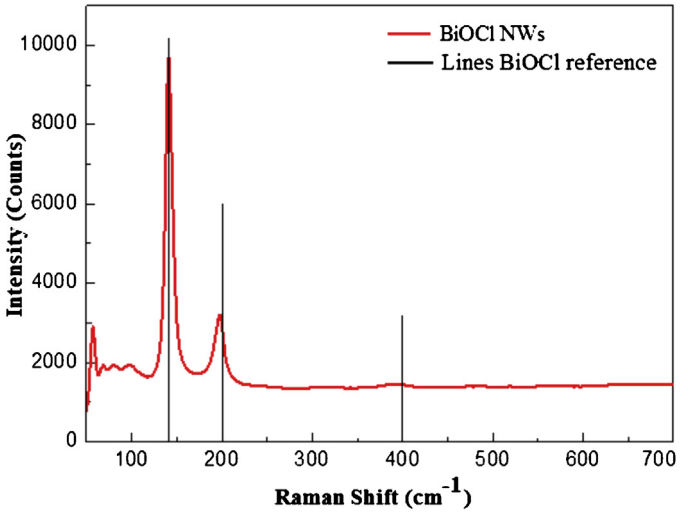

Fig. 3. Low energy micro-Raman analysis on BiOClNWs deposited on silicon wafers and BiOCl reference lines.

Table 2
BiNWs thickness and elemental composition on different substrates by EDS.

No.	Silicon wafer type	Thickness (nm)	Stoichiometric composition (wt.%) (±1%)		
			Bi	Cl	O
1	Silicon (100)	44–237	80	11	7
2	Silicon (111)	27–77	76	12	11
3	Silicon carbide (SiC)	73–180	80	11	7

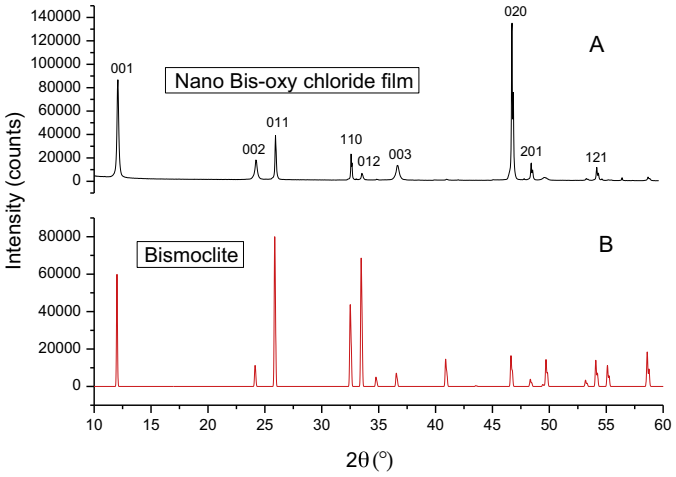

Fig. 4. XRD of, (a) BiOClNWs obtained in the present work for the sample deposited on Si (111), (b) Bismoclite in powder form.

3.4. X-ray diffraction (XRD)

As shown in Fig. 4a, the XRD pattern exhibits intense, sharp peaks. The narrow broadening of the peaks is consistent with the size of nanocrystallites evidenced by FESEM images (Table 1). For the phase identification, we compared the generated diffraction pattern to the ICDD database using Bruker EVA software. The occurrence of intense peaks indicates that the film is highly crystallized. Notice that the main peak around $2\theta = 47.1^\circ$ is due to the silicon substrate.

The other peaks have been assigned to the known XRD data for powder BiOCl [30] (PDF number 01-073-2060) that crystallizes in a tetragonal structure with P 4/nmm Space Group (Fig. 4b). The crystal structure can be thought of as consisting of layers of Cl^-, Bi^{3+} and O^{2-} ions, in the order [—Cl—Bi—O—Bi—Cl—Cl—Bi—O—Bi—Cl—]. The bismuth atoms adopt a square antiprismatic order with four chlorine atoms forming one of the square faces, and four oxygen atoms forming the other square face. Comparing Fig. 4a and b, it is noticed that the films presented preferred orientation, no random as the Bismoclite powder, which is consistent with the SEM images, that showed the nano-platelets clearly oriented.

3.5. X-ray photoelectron spectroscopy (XPS)

XPS analysis was performed on the as-grown film (Fig. 5a) and after having it sputtered with an Ar flux for 13 min at 2 kV (Fig. 5b), in order to remove surface contaminations. The Survey spectrum before sputtering (Fig. 5a) shows four main photo-electronic peaks, O_{1s}, C_{1s}, Cl_{2p} and Bi_{4f}: their relative atomic concentrations were evaluated after subtracting the background with a Shirley function (Table 3). After sputtering, the C_{1s} peak disappeared, due to the surface contamination removal. High resolution (HR) spectra of these peaks was decomposed using Voigt functions in order to evaluate the chemical bonding state. After an exhaustive research in the literature [31,32] the peaks were attributed to different chemical bonds as reported in Table 3. Bi peak is made up by the superposition of three peaks: at 156.9 eV assigned to Bi metallic form, at

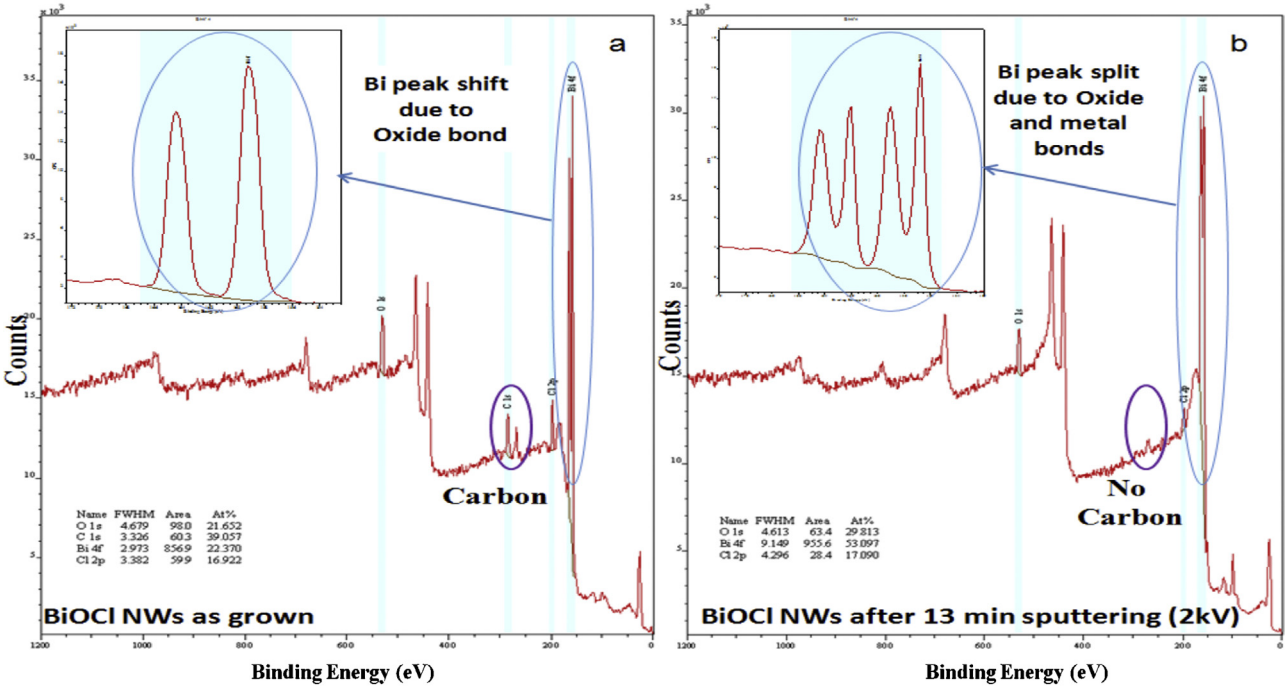

Fig. 5. XPS survey spectrum of BiOClNWs (a) as grown (b) after sputtering for 13 min.

Table 3
XPS Elemental quantification and peak deconvolution of BiOClNWs as grown and after sputtering.

Element	Quantification (%)(±0.1%)		Peak (eV) (±0.2%)	Atomic Wt.% (±0.1%)		Bond
	As grown	Sputtering		As grown	Sputtering	
O_{1s}	21.7	29.8	529.8	50.1	53.6	BiOCl
			532.2	35.5	46.4	Bi_2O_3
			532.9	14.3	–	C—O—C
C_{1s}	39.0	–	284.6	82.5	–	C—C (graphite)
			286.5	17.5	–	C—O—C
$Bi_{4f7/2}$	22.4	53.1	156.9	5.1	33.9	Bi metal
			157.4–158.6	33.9	20.3	Bi_2O_3
			159.0–159.4	61.0	45.8	BiOCl
$Cl_{2p3/2}$	16.9	17.1	197.9	100	100	BiOCl

157.4–158.6 eV assigned to Bi_2O_3 and the latter at 159.0–159.4 eV assigned to BiOCl. The same procedure has been repeated for the sputtered sample, as reported in Fig. 3b, obtaining the results mentioned in Table 3. After the removal of the surface contamination, the Bi amount is consequently increased, thanks also to the reduction of the oxide compounds.

4. Conclusion

In this paper, we have shown that bis-oxy chloride (BiOCl) nano walls can be synthesized in thin film form on a variety of substrates using a MOCVD technique. Compared to conventional solution techniques, the solution dispersion method is extremely simple, effective and easy to scale up. Micrometre thick films formed by 20–240 nm thick nanosheets of crystalline bis-oxy chloride (BiOCl) were deposited it was observed that the nanowall thickness depended on the substrate, however, the reason is not clear yet. The relationship between substrate surface orientation, micro-roughness, surfaces energy and the BiOCl growth will be very important to understand. The clear background and peak width in XRD shows the BiOCl NWs are crystalline without much contamination which is better than any other conventional method used to prepare the BiOCl NWs. More detailed and systematic studies are currently under way in an effort to provide more insight into the properties of this material and achieve a better tailoring of thin films.

Acknowledgments

This research has been financially supported by Bisnano, a Collaborative Project between Europe and Mexico (FP7-NMP-2010-EU-Mexico) Project Number: EU 263878, CONACYT 125141. We thank Dr. Salvatore Guastella (Polytechnic of Turin, Italy) for valuable discussion.

References

[1] S.N. Irwing, R.J. Bewis, Dangerous Properties of Industrial Materials, Van Nostrand Reinhold, New York, 1989.
[2] U. Wormser, I. Nir, The Chemistry of Organic Arsenic, Antimony and Bismuth Compounds, Wiley, New York, 1994.
[3] J. Reglinski, Chemistry of Arsenic, Antimony and Bismuth, Blackie, London, 1998, pp. 403–440.
[4] N. Gunnar, Handbook on the Toxicology of Metals, Academic Press, Inc., Waltham, 2007.
[5] S. Cao, C. Guo, Y. Lv, Y. Guo, Q. Liu, Nanotechnology 20 (27) (2009) 275702.
[6] D. Berlincourt, J. Acoust. Soc. Am. 91 (5) (1992) 3034–3040.
[7] Z. Deng, D. Chen, B. Peng, F. Tang, Cryst. Growth Des. 8 (8) (2008) 2995–3003.
[8] Z. Deng, F. Tang, A. Muscat, Nanotechnology 19 (2008) 1–6.
[9] H. Völz, Ullmann's Encyclopedia of Industrial Chemistry, John Wiley & Sons, USA, 1999, pp. 120–121.
[10] L. Zhu, Y. Xie, X. Zheng, X. Yin, X. Tian, Inorg. Chem. 41 (17) (2002) 4560–4566.
[11] C. Wang, C. Shao, Y. Liu, L. Zhang, Scr. Mater. 59 (3) (2008) 332–335.
[12] M. Postel, E. Dunach, Coord. Chem. Rev. 155 (1996) 127–144.
[13] C. Nayral, T. Ould-Ely, A. Maisonnat, B. Chaudret, P. Fau, L. Lescouze'res, A. Peyre-Lavigne, Adv. Mater. 11 (1) (1999) 61–63.
[14] S. Chai, Y. Kim, M. Jung, A. Chakraborty, D. Jung, W. Lee, J. Catal. 262 (2009) 144–149.
[15] X. Zhang, X. Liu, C. Fan, Y. Wang, Y. Wang, Z. Lian, Appl. Catal. B: Environ. 132–133 (2013) 332–341.
[16] S. Wua, C. Wangb, Y. Cui, Appl. Surf. Sci. 289 (2014) 266–273.
[17] K. Zhang, C. Liu, F. Huang, C. Zheng, W. Wang, Appl. Catal. B: Environ. 68 (2006) 125–129.
[18] J. Aran˜, P. Piscina, J. Llorca, J. Sales, N. Homs, J. Fierro, Chem. Mater. 10 (1998) 1333.
[19] S. Majetich, Y. Jin, Science 284 (1999) 470.
[20] D. Gittins, D. Bethell, D. Schiffrin, R. Nichols, Nature 408 (2000) 67.
[21] J. Zhou, Z. Wu, Z. Zhang, W. Liu, Q. Xue, Tribol. Lett. 8 (2000) 213.
[22] M. Bonini, U. Bardi, D. Berti, C. Neto, P. Baglioni, J. Phys. Chem. B 106 (2002) 6178.
[23] R. Andres, J. Bielefeld, J. Henderson, D. Janes, V. Kolagunta, C. Kubiak, W. Mahoney, R. Osifchin, Science 273 (1996) 1690.
[24] F. Mafuné, J. Kohno, Y. Takeda, T. Kondow, J. Phys. Chem. B 106 (2002) 7575.
[25] J. Yu, B. Wei, L. Zhu, H. Gao, W. Sun, L. Xu, Appl. Surf. Sci. 284 (2013) 497–502.
[26] Y. Cui, Q. Jia, H. Li, J. Han, L. Zhu, S. Li, Y. Zou, J. Yang, Appl. Surf. Sci. 290 (2014) 233–239.
[27] Y. Zhao, Z. Zhang, H. Dang, Mater. Lett. 58 (2004) 790–793.
[28] O. Kharissova, M. Osorio, B. Kharisov, M. Yacamán, U. Méndez, Mater. Chem. Phys. 121 (2010) 489–496.
[29] J. Zhang, J. Xia, S. Yin, H. Li, H. Xu, M. Hea, L. Huanga, Q. Zhang, Colloid. Surf. A: Physicochem. Eng. Aspect. 420 (2013) 89–95.
[30] B. Downs, Database RRUFF Project, Department of Geosciences, University of Arizona, 2005.
[31] C. Wang, C. Shao, Y. Liu, L. Zhang, Scr. Mater. 59 (2008) 332–335.
[32] V. Simon, M. Todea, A.F. Takács, M. Neumann, S. Simon, Solid State Commun. 141 (2007) 42–47.